ELSEVIER

Biophysical Chemistry 65 (1997) 123–141

Biophysical Chemistry

Ion–water and water–water interactions in a gramicidinlike channel: effects due to group polarizability and backbone flexibility

Karen A. Duca [a], Peter C. Jordan [a,b,*]

[a] *Program in Biophysics, Brandeis University, South Street, Waltham, MA 02254 USA*
[b] *Department of Chemistry, Brandeis University, South Street, Waltham, MA 02254 USA*

Received 8 July 1996; revised 10 September 1996; accepted 10 September 1996

Abstract

In the gramicidin channel, ionic transport and water transport occur simultaneously. Gramicidin's transport properties are influenced by ionic interactions with both the polypeptide and the channel waters. We present results of molecular dynamics studies on a series of alkali metal ions interacting with a water-filled gramicidinlike channel (a configurationally constrained polyglycine analog) at the dimer junction, in mid-monomer, and near the channel entrance. We investigate details of both short and long range ion–water and water–water correlation; these are notably dependent on the explicit consideration of polarizability and the degree of backbone flexibility. The nature of ion–water and water–water correlations changes as ionic size decreases and these changes may be augmented or attenuated by manipulation of the two parameters under study. Incorporating polarizability generally shortens ion–water distances and enhances ion-induced electrostriction (decreased water–water separations), while simultaneously reducing the long range orientational correlation of the single filing waters within the channel. Increasing flexibility predictably results in a broadening of the distribution of water–water and ion–water separations and contributes to the loss of long range orientational correlations. Both effects are ion specific; Cs^+ and Na^+ interact with the channel in distinctly different ways, while K^+ represents an intermediate case more closely resembling Cs^+. Our results demonstrate that incorporation of polarizability in the potential function has significant effects on the properties of channel water and, consequently, on the ionic transport process. While ion–water and water–water distances are decreased due to this feature, thereby fostering longer ranged correlations within the channel, enhanced interactions between water molecules and peptide groups tend to mitigate this effect. Possible implications for the multiple occupancy states of gramicidin and long range information transfer via a single file water chain are considered. © 1997 Elsevier Science B.V.

Keywords: Model channel; Gramicidin; Polarizability; Membrane fluidity

1. Introduction

A number of questions are central to developing a theoretical understanding of the mechanism by which transmembrane ion channels catalyze the transfer of

* Corresponding author. Tel.: 1 617 7362540; Fax.: 1 617 7362516; e-mail: jordan@binah.cc.brandeis.edu.

PII S0301-4622(96)02233-8

ions across the lipid bilayer. Among the most challenging is the issue of how and when the channel permits entry of certain ions and exclusion of others. The qualitative features that must account for biological ion channels' exceptional ability to selectivity facilitate translocation of ions across membranes have often been described [1]. Narrow pore interiors, lined with polar or charged groups, in which permeant motion proceeds in a single file, provide an environment which stabilizes water and some charged species. Selectivity rests upon a delicate energetic balancing between rather large binding energies [2–6]. The relative affinity of an ion for water and the channel interior can not differ too much; furthermore, the energy barriers to ion entry, exit, or translocation can not be too great. If these conditions are not satisfied, an ion can not permeate; it will either block the channel or not enter it at all. In addition to facilitating ionic translocation across the membrane, certain channels also permit signal transduction either along or across membranes [7]. The nature of the signal transduced may depend, either directly or indirectly, on the identity of the ion transported.

Physiologically active channels are typically composed of multiple integral membrane protein subunits arranged around the aqueous permeation pathway; they frequently have several thousand amino acid residues. Despite knowledge of the primary sequences of the constituent subunits, relatively few high resolution structural data are available. Indeed, no internal structure of a biologically significant channel is known to better than 9.0 Å resolution [8]. Theoretical studies of ion permeation at the molecular level have of necessity focused on simpler channel forming proteins. The pentadecapeptide gramicidin A and its analogs are small channel forming peptides, readily amenable to chemical modification, and relatively easily studied electrophysiologically [9–11]. Questions of general applicability to the important physiological channels notwithstanding, gramicidin A and its various analogs are excellent systems for the theoretical investigation of ion translocation [12–16,4,17]. Among its more striking properties is the fact that, depending upon which alkali cation is transported, it can be either doubly (Cs^+, Rb^+, or K^+) or singly (Na^+ or Li^+) occupied at high (> 1 M) permeant ion concentration [18]. This behavior is interesting since the ionic binding sites are located near the mouths of the channel, approximately 19 Å apart [19–21]. Assuming that both binding sites exhibit an equal intrinsic affinity for a particular ion, the dielectric constant, ε, within the aqueous channel would have to be approximately 4 in order for electrostatic repulsion alone to account for the difference between the observed first and second affinity constants [18]. While $\varepsilon \sim 4$ is consistent with previous theoretical estimates [22], the actual dielectric properties of the channel interior are unknown. Obviously, as the ion enters the mouth of the channel, membrane and protein motions, as well as ion–side chain interactions, alter the ionic field [23,24]. Therefore, there remain questions as to whether an ion entering on one side of the channel can distinguish between the influence of different alkali cations bound at the opposite side. To investigate these questions one must consider how the different ions interact with the channel waters and/or the polypeptide and how they propagate occupancy information across the entire channel length.

The water chain has been investigated theoretically as a means by which this information may be transmitted along the channel. Chiu and co-workers [15,25,26] consider the single file waters, as well as some of their hydrogen bonding peptide partners, as a collective chain whose transitions between conformations are highly correlated. Extending this concept even further, Poxleitner et al. [27] define the external capping water, the polypeptide, and the channel waters as the functional unit of gramicidin A. Roux et al. [28], building on prior studies of the energetics and dynamics of various model channels [16,4,17,29], conclude that the trend toward higher occupancy in gramicidin arises from the loss of favorable long-range ion–water chain interactions, with water–channel interactions also playing a role. In order to describe the many body character of the ionic transport process, Elber et al. [30] define a quasi-particle called a 'permion' which consists of a plug of waters accompanied by an ion. In their model forward motion proceeds in a highly correlated manner involving a reptation mechanism whereby the permion is nudged along the channel by helix motions. Although experimental validation of conclusions based on these models is not easily obtainable, measurements of magnetic field strength dependent spin-

lattice relaxation have established the existence of nanosecond librational motions along the channel axis which coincide with ionic transit times [31,32].

This paper presents a study of the effects that cation variation, backbone flexibility, and group polarizability have on the properties of channel water with special attention paid to those factors which might account for long range information transfer and its indirect implications for channel selectivity. Our computations yield structural data illustrating how cation identity, backbone rigidity or fluidity, and polarizable groups influence the pore waters' electrical properties, water–water, and ion–water correlations. A detailed study of ion–helix and water–helix interactions in the mid-monomer highlighting energetics as well as structural features is currently under way and will be presented in a later paper.

2. Model and theory

The structure of the predominant electrically active form of gramicidin A in oriented bilayers has been elucidated by NMR spectroscopy [33–37]. The model employed here, however, is a more simplified polyglycine analog of the head-to-head dimer which incorporates major qualitative features essential to understanding gramicidin's electrical conductance [38–41]. Given its narrow diameter and lack of interior side chains, the polar groups of the gramicidin backbone must assume the primary responsibility for the transport of ions through the pore. Consequently, a model constructed strictly of glycine will replicate critical features of ionic translocation with a few caveats. For example, experimental work suggests that the tryptophans near the mouth of the channel are rather important for modulation of gramicidin conductance, perhaps by deforming the binding sites [42]. Although the side chains do not project into the channel lumen, their modification has been shown to result in measurable changes in channel conductance [43,11]. Conformational analysis provides a reasonable set of coordinates for the backbone atoms of the model channel [44]. This is a left-handed structure, while gramicidin A is actually right-handed [33–37]. However, as left and right handed versions of the polyglycine analog are mirror images, this choice has no energetic or structural consequences. Moreover, the channel is idealized for the purpose of highlighting the influence of the two key parameters and handedness does not change the interpretation of our results. Monomers are joined at the N-termini via 6 interhelical hydrogen bonds. The CHO group at the N-terminus is numbered 0 and the COH of the ethanolamine tail is numbered 16. All but six carbonyl oxygens (numbered 11, 13, 15, 11′, 13′, and 15′) form intra- or inter-monomer hydrogen bonds. (See Fig. 1)

The model geometry is similar to that described previously [45,40]. In the present study, bulk water is approximated by hemispherical caps of radius 11.5 Å at each end of the channel; about 40 water molecules are in each cap. Water remains within the boundary

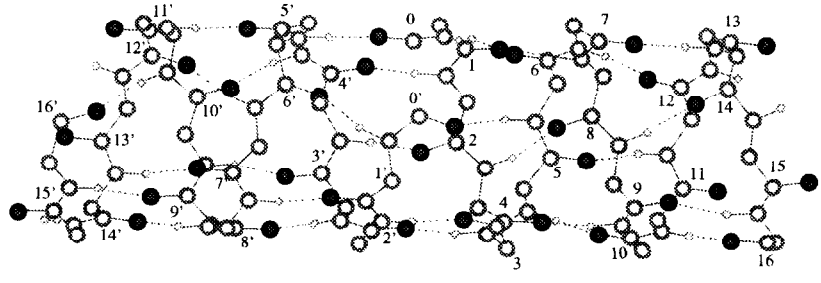

Fig. 1. Projection of the β-helical backbone of the polyglycine analog of the dimeric gramicidin channel. The coordinates employed are those calculated by Koeppe and Kimura [44]. The filled circles are the oxygen atoms of the CO moieties; the small circles are the hydrogen atoms of the NH groups; the unliganded circles are C_α groups. Numbers 1–15 refer to the corresponding amino acids of the first pentadecapeptide monomer. Number 0 is the formyl CO and number 16 is the ethanolamine carbon. Numbers 0′–16′ designate the equivalent units on the second monomer. Only hydrogen atoms of the NH moieties are depicted. The dotted lines represent hydrogen bonds between CO and NH groups. Reprinted by permission of ACS [39].

of the hemispherical wall by damping the velocities of escaping molecules. Particles slipping through the sides of the caps into the lipid region are simply reflected elastically. The H_2O density in the cap domains is variable but approximately that in bulk water. Reducing the number of bulk water molecules substantially reduces the computational demands from that required in the previous studies which included 418 water molecules. By comparison with simulations on Cs^+ (Jordan, unpublished results) this truncation has no significant effect on ion–channel–water properties in the regions of interest. As was done previously, the channel is embedded in a lipid-like domain of 589 randomly distributed immobile, non-polarizable force centers for the rigid channels and 560 such centers for the flexible and very flexible ones. These spheres are roughly the size of CH_2 groups and occupy a cylindrical region of 15 Å radius around the model gramicidin dimer. They do not have the chain-like order found in lipid bilayers, although the number density approximates the CH_2 group density in stearic acid. The interaction between the immobile spheres and all other groups is a Lennard–Jones potential with $\varepsilon = 0.59$ kJ mol^{-1} and $\sigma = 3.46$ Å, typical of a CH_2–water interaction [46].

The model and the theoretical procedures used have been described in detail in previous work [40]; we give a summary here, omitting only a description of the switching function used and the Lennard–Jones parameters for our groups. The potential energy function contains five terms: electrostatic, Lennard–Jones, bond polarization (responsible for creating the induced dipoles), backbone deformation (accounting for the structural deformations due to thermal motions, i.e., bond stretching, bond bending, and amide plane deformation), and group localization contributions [38,41,45,46]. It differs from standard biomolecular force fields such as CHARMM [47], AMBER [48], or GROMOS [49] in two significant ways: the basic units are uncharged, multipolar or dipolar moieties (H_2O, CO, NH), rather than individual atoms and each of our groups is polarizable. We can thus treat charge redistribution due to ion–group and group–group interactions, which has been found to be very important in the pore environment [50,29]. In our calculations, pathological configurations giving rise to 'polarization catastrophes' never arise; the short range repulsion terms in the various potentials are sufficient to keep any pair of molecules from approaching too closely, so dipole moments never diverge.

We use a polarizable electropole model for water [51,52]. It has the electrical moments and the polarizability of an isolated water molecule; the short range Lennard–Jones repulsive term is parameterized to account for properties of the water dimer. This model adequately describes water's second virial coefficient, many properties of small water clusters, and the energetics of ice Ih. It is less successful in treating liquid water; the binding energy is too small and both X-ray and neutron pair distribution functions are only qualitatively reproduced. However, for the purpose of analyzing the influence of the polarizability of channel water in a single file environment (large water clusters can not form), it represents a good compromise. It should be noted that currently no single potential function accurately describes the properties of water in a wide range of phases. Furthermore, it has been suggested that the channel contents have properties similar to supercooled bulk water and ice [25,26]. The Barnes potential, which is relatively better at describing the energetics of ice Ih than liquid water, provides a reasonable model for a hybrid system such as channel H_2O. The ion–water potentials were parameterized to fit the properties of ion–water microclusters [53,54]; again this emphasizes short range structural features, precisely what is required in a channel.

To examine the significance of including polarizability (permitting dipole moment fluctuations), we also consider a potential function modified in the following way. In the studies with polarizability in the potential function, electrostatic interaction increases the mean dipole moments of the various groups (CO, NH, and H_2O); they are naturally significantly larger than their bare (non-interacting) values. To carry out a comparable study excluding polarizability requires increasing the group dipole moments; the values chosen were the mean values determined in simulations where $\alpha > 0$ [40]. The adjusted moments are: CO: 2.56 D; NH: 1.08 D; bulk H_2O: 2.47 D (the same as Barnes' value [50]); channel H_2O: 2.31 D. We used different values for the channel and bulk waters because, as shown in earlier studies [40], the channel and bulk environ-

ments affect water polarization in significantly different ways. Bulk water is far more effectively polarized and this is reflected in the larger dipole moment. The dipole moment of the channel water was assigned based on simulations in channels containing only water molecules. We refer to simulations with polarizability in the potential function as $\alpha > 0$ simulations, while those with fixed dipole moments are identified as $\alpha = 0$ simulations.

Water, the groups of the gramicidin backbone, and the ion are described as polarizable multipoles embedded in Lennard–Jones spheres. The relevant parameters are given elsewhere [40]. As already indicated, the capping water is treated slightly differently from channel water in the $\alpha = 0$ simulations to account for differences in the two environments. Within the gramicidin monomers the forces, torques, and electric fields depend on the interaction between all groups separated by less than a preselected cut-off distance; however, near neighbors in a particular monomer are not coupled via the non-bonded forces (electrostatic and Lennard–Jones).

The group localization energy term is included to stabilize monomer helices during dynamics to partially compensate for the fact that side chains are not included in the treatment. Cohesive forces arising from interactions between amino acid residues or between peptide side chains and lipid, while important for structural stability, are ignored. As a result, an additional constraint is needed to maintain helicity near the channel entrance [40] and to insure that all six hydrogen bonds form at the junction. As a surrogate for membrane fluidity we consider three degrees of helical flexibility for our study, viz. rigid, flexible, and very flexible backbones. We achieve the various degrees of flexibility by modification of the force constant for the harmonic restoring force associated with the group localization energy term $(\Sigma 0.5k(r_i - r_{0i})^2$, where r_{0i} is the 0 K position of group i). The force constant k was varied from 5 to 0.01 mdyne nm^{-1}; the latter value corresponded to channel closure, as groups occluded the permeation pathway. Data are reported for all backbone flexibilities where the channel remained open during the entire simulation. Rigid channel backbone groups are highly localized to their 0 K positions with an rms displacement equal to 0.10 Å. The flexible channels exhibit an rms displacement of 0.29 Å from the 0 K positions, while the very flexible channels are highly delocalized with an rms displacement of 0.64 Å. The absolute degree of backbone flexibility for any type of actively conducting ionic channel is still an unanswered question, although there is suggestive experimental evidence that gramicidin is relatively more, rather than less rigid [55–57].

As the ion is translated through the channel, umbrella sampling is used to link neighboring regions. In a single simulation we begin with a starting configuration located near an energy minimum or maximum and move the ion a total of 1.0–1.6 Å through the channel up to or beyond the next local maximum or minimum, respectively. Upon completion of the calculation at one location the ion is translated in the channel to its next location and the process repeated. As the potential changes rather rapidly for smaller ions like Na^+, the windows are separated by only 0.1 Å for all flexible and very flexible channels. In the case of the rigid channel, the windows for K^+ and Na^+ are separated by 0.1 Å, while those for Cs^+ are separated by 0.2 Å.

As mentioned, a cut-off was used; particles are fully interacting at 8.5 Å and out of range at 9.5 Å. Extending this cut-off to 12 Å in a selected region did not result in significant changes in the averages of properties studied. Future studies of ion–helix correlations in the mid-monomer will extend the cut-off to examine the importance of long-range interactions as the ion changes its coordination between a maximum and a minimum. Temperature control is maintained by Langevin coupling with a relaxation time of 0.1 ps [58]. A 5 point Gear predictor–corrector method is used to solve the equations of motion [59]. Rotational coordinates are described by Cayley–Klein parameters [60]. Moments of inertia are increased: for the polar groups of the helix, 10-fold and for water, 100-fold. This slows down the rate of water, CO, and NH rotation and facilitates rotational energy transfer, which can have no effect on equilibrium properties but permits relatively large time steps (2 fs) to be used in the calculation, further reducing the computer time required. Each starting configuration was annealed for at least 2.5 ps at 400 K and 2.5 ps at 350 K, followed by at least 15 ps of equilibration at 300 K. In each window the system was re-equilibrated for 5 ps and data collected for the subsequent 10 ps for the

rigid channel, 40 ps for the flexible channel, and 20 ps for the very flexible channel. Both flexible and very flexible channels reached equilibrium by 20 ps. We continued the simulations on the flexible channels for an additional 20 ps to reduce statistical variation, as we expect that this degree of flexibility most nearly approximates experimental conditions. Channels containing only water were subjected to the same thermalization and equilibration procedure; however, without an ion to promote ordering, longer annealing and equilibration times were required. The annealing times were 5.0 ps at each elevated temperature, followed by at least 60 ps equilibration. Data were then collected for 120 ps for all degrees of flexibility.

Two types of test were used to check that sampling was adequate. Data collected in the first half of the run were not statistically different from the results collected during the second half. Occasionally an intermediate window configuration was re-annealed and re-equilibrated before sampling; the data collected after this procedure were not significantly different from results found without the re-annealing. Potassium required more careful equilibration at the start in each region; in the very flexible channel at the mid-monomer the system was equilibrated for at least 20 ps before data collection. In the absence of this extended procedure, excessively large gaps ($>$ 3.7 Å) sometimes arose in the water chain. In fact, transiently rather large gaps (3.5 Å $<$ distance$_{w-w}$ $<$ 3.7 Å) did occur, especially when the K^+ was near a local energy maximum. We attribute this phenomenon to potassium's inability to either execute large off-axis motions (like sodium) or to be fully solvated while remaining on-axis during its trajectory through the channel (like cesium). Potassium behaves sometimes like sodium and sometimes like cesium as it traverses the channel, influenced by its initial configuration.

3. Results

We contrast properties of Na^+, K^+, and Cs^+ occupied channels. From the structure of the gramicidin molecule, four distinct binding regions can be identified in each half of the channel (See Fig. 1): the mouth, in which the ion binds with CO number 11 and the ethanolamine COH and still maintains most of its hydration shell; the entrance to the single file, in which the ion associates most strongly with CO's number 9 and 14; the interior (mid-monomer), in which the ion moves successively among pairs of CO's 7 and 12, 5 and 10, 3 and 8, 1 and 6; and the junction, where it associates with carbonyls numbered 0′, 2′, 2, and 4. Within the channel ions are solvated by two waters of hydration and by carbonyl groups forming the channel interior. We describe general properties of the non-exchangeable, single file waters as the ion traverses the membrane within the model gramicidin channel, highlighting stretches of 1.0 to 1.6 Å along the main channel axis in regions designated as the junction, mid-monomer, and exit (entrance to the single file and mouth, as above). Non-exchangeable waters are defined as those molecules which remain in the channel for the entire duration of the simulation. At extremities of the channel (ca. 10.5 Å from the junction), the last water molecule occasionally switches places with a bulk H_2O; these exchangeable molecules are not included in our analysis.

3.1. Water dipole moments

Table 1 presents mean water dipole moments in the unoccupied channel (μ_{free}) and for those water molecules which are first and second nearest neighbors (μ_{w_1} and μ_{w_2}) of the ion in various regions of the occupied channel. Some general patterns are apparent. In each model channel there is no statistically significant difference between μ_{w_1} in the different channel regions; however, when taken as a whole, the trends in the more flexible channels suggest that μ_{w_1} is smaller when the ion is near the channel exit. Similarly, in the most flexible channel, there appears to be regional variation of μ_{w_2}, with μ_{w_2} being smallest when the ion is near the channel exit. It is again unclear if this is statistically significant.

The influence of backbone flexibility is self-evident. For the smallest ion, Na^+, μ_{w_1} is unmistakably lower when the channel is made more flexible; moreover, there is a fairly large and statistically significant difference between μ_{w_2} and water's mean dipole moment in ion-free channels. K^+ behaves in a similar fashion, but the dependence of μ on channel flexibility is less pronounced. The dipole moment of

Table 1
Mean channel water dipole moments [a]

	Na^+		K^+		Cs^+	
	μ_{w_1}	μ_{w_2}	μ_{w_1}	μ_{w_2}	μ_{w_1}	μ_{w_2}
Rigid channels, $\alpha > 0$ ($\mu_{free} = 2.30 \pm 0.03$)						
Junction	2.93 ± 0.03	2.49 ± 0.03	2.64 ± 0.03	2.41 ± 0.03	2.53 ± 0.02	2.40 ± 0.04
Monomer	2.93 ± 0.03	2.49 ± 0.05	2.64 ± 0.06	2.39 ± 0.07	2.54 ± 0.04	2.39 ± 0.04
Exit	2.90 ± 0.04	2.50 ± 0.07	2.66 ± 0.05	2.40 ± 0.07	2.49 ± 0.03	2.32 ± 0.05
Flexible channels, $\alpha > 0$ ($\mu_{free} = 2.32 \pm 0.02$)						
Junction	2.84 ± 0.03	2.48 ± 0.03	2.56 ± 0.03	2.37 ± 0.03	2.48 ± 0.03	2.32 ± 0.04
Monomer	2.85 ± 0.04	2.46 ± 0.05	2.54 ± 0.06	2.37 ± 0.03	2.48 ± 0.02	2.35 ± 0.02
Exit	2.79 ± 0.02	2.40 ± 0.02	2.53 ± 0.04	2.34 ± 0.04	2.48 ± 0.03	2.33 ± 0.03
Very flexible channels, $\alpha > 0$ ($\mu_{free} = 2.33 \pm 0.02$)						
Junction	2.73 ± 0.03	2.46 ± 0.06	2.58 ± 0.02	2.38 ± 0.07	2.52 ± 0.04	2.43 ± 0.05
Monomer	2.73 ± 0.05	2.41 ± 0.07	2.54 ± 0.06	2.39 ± 0.07	2.47 ± 0.03	2.33 ± 0.02
Exit	2.74 ± 0.03	2.42 ± 0.05	2.50 ± 0.04	2.33 ± 0.05	2.48 ± 0.04	2.33 ± 0.03
Cation–water clusters						
MW_2^+	2.84		2.68		2.53	
MW_4^+	2.58		2.47		2.39	
MW_6^+	2.43		2.36			

[a] The dipole moments (in Debye) for the first (μ_{w_1}) and second (μ_{w_2}) nearest neighbor water molecules were averaged for Cs^+, K^+, and Na^+ occupied channels. μ_{free} is the mean channel water dipole moment in the unoccupied channel. Dipole moment values computed for gaseous cation–water microclusters [54] are given for comparison.

the second nearest neighbor is still somewhat larger than μ_{free}. By the time the ionic radius equals that of Cs^+, both μ_{w_1} and μ_{w_2} are independent of channel flexibility; furthermore, μ_{w_2} differs little from μ_{free}. With Na^+ in the channel the water dipole moment is markedly sensitive to the degree of channel flexibility, but this effect disappears as ionic radius increases. In contrast, in the water only simulations μ_{free} is little affected by the degree of flexibility of the channel and increased flexibility serves, if anything, to increase μ_{free}.

Parallels can be drawn between these μ values and those computed for water in gaseous cation–water (MW_x^+) microclusters. In the case of μ_{w_1} for rigid channels occupied by sodium, the MW_2^+ water dipole moments are actually lower than those found in the model channel. For the flexible channels they are approximately the same and for the very flexible channels they are higher. In the case of the potassium occupied channel the MW_2^+ water dipole moments are equal to μ_{w_1} in the rigid channel and slightly higher than those of the flexible and very flexible channels. For cesium the μ_{w_1} values are approximately the same as those of the gaseous cation–water dimer for all flexibilities. A drop in water dipole moments is not surprising as a consequence of increasing flexibility, reflecting the fact that water molecules are less constrained. It is curious that the μ_{w_1} for the rigid sodium-occupied channel is higher than the water dipole moment in MW_2^+ and this may suggest that within the rigid channels water is very highly constrained indeed, enhancing its polarization. This interpretation is consistent with MD simulations of water-filled gramicidin channels by Chiu et al. [15], where H_2O molecules became 'frozen' in rigid channels. The values of μ_{w_2} are all noticeably smaller than μ_{w_1}, indicating that these waters are part of a second hydration shell.

3.2. Ion–water correlations

The average number of waters that are co-transported with an ion through the channel depends on

channel flexibility, group polarizability, and ionic size. Co-transported waters are those waters which the ion is able to restrain within the channel for the duration of a simulation, i.e., non-exchangeable waters. There are more non-exchangeable waters found in all channel regions when the backbone remains rigid. In this case, sodium and potassium transport eight waters, while cesium transports seven. For the more flexible channels, $\alpha > 0$ tends to favor retention of water, but only for the smallest ion. Sodium carries seven waters through the channel when $\alpha = 0$ and eight when $\alpha > 0$. Potassium transports 6.7 and cesium, 6.3, independent of polarizability. By the time the channel reaches the very flexible state all three ions exhibit only small differences between the $\alpha = 0$ and $\alpha > 0$ cases. Sodium occupied channels in $\alpha = 0$ simulations contain an average of 6.6 waters. Equivalent channels with $\alpha > 0$ contain about seven waters. To summarize, increasing backbone flexibility or ionic size reduces the number of waters that remain in the channel with an ion. Dynamical polarizability only increases the number of waters when the channel is flexible and the ion is small.

These results are consistent with both the experimentally derived values and theoretical results reported by other groups. At low permeant ion concentration (< 1 M), seven to nine waters accompany the larger ions through the channel [61–63] and this number drops to five at high ionic concentration. Sodium, however, always transports nine waters, independent of concentration. In earlier simulations [12,64,3] the occupancy numbers are similar to our rigid, $\alpha > 0$ type observations. The channel model employed by Skerra and Brickman [3] is most like the one used here, while that of McKay is most different. Skerra and Brickman represent gramicidin by a hexagonal arrangement of CO group like-dipoles possessing three vibrational modes (in- and out-of-plane bending and bond stretching). The carbon atoms are fixed on a rigid helix, making their model similar to our rigid backbone. Water–water interactions are described by the TIP4P model. They

Table 2
Mean ion–water separations (in Å) for nearest water neighbors [a]

	Na^+		K^+		Cs^+	
	$\alpha = 0$	$\alpha > 0$	$\alpha = 0$	$\alpha > 0$	$\alpha = 0$	$\alpha > 0$
Rigid						
Junction	2.53 ± 0.03	2.48 ± 0.03	2.92 ± 0.03	2.88 ± 0.03	3.19 ± 0.03	3.17 ± 0.05
Monomer	2.52 ± 0.02	2.47 ± 0.03	2.90 ± 0.03	2.87 ± 0.03	3.15 ± 0.02	3.14 ± 0.03
Exit	2.52 ± 0.04	2.48 ± 0.02	2.88 ± 0.03	2.86 ± 0.03	3.17 ± 0.03	3.18 ± 0.04
Flexible						
Junction	2.56 ± 0.05	2.48 ± 0.03	2.94 ± 0.03	2.91 ± 0.03	3.18 ± 0.04	3.17 ± 0.03
Monomer	2.56 ± 0.03	2.48 ± 0.03	2.92 ± 0.03	2.88 ± 0.03	3.16 ± 0.03	3.16 ± 0.03
Exit	2.53 ± 0.04	2.47 ± 0.04	2.91 ± 0.02	2.90 ± 0.04	3.18 ± 0.04	3.15 ± 0.03
Very flexible						
Junction	2.59 ± 0.04	2.49 ± 0.05	2.95 ± 0.05	2.88 ± 0.06	3.20 ± 0.04	3.18 ± 0.05
Monomer	2.61 ± 0.04	2.53 ± 0.05	2.92 ± 0.03	2.90 ± 0.05	3.19 ± 0.06	3.17 ± 0.06
Exit	2.59 ± 0.02	2.52 ± 0.04	2.92 ± 0.03	2.93 ± 0.06	3.16 ± 0.04	3.14 ± 0.04
Cation–water clusters						
MW_2^+	2.52		2.78		3.11	
MW_4^+	2.57		2.83		3.18	
MW_6^+	2.62		2.87			

[a] Ion–water distances computed for gaseous cation–water microclusters [54] are given for comparison.

find that the sodium channel is occupied by eight water molecules, while potassium contains only seven, which is, not unexpectedly, identical to our rigid simulations. McKay et al. [12] use a full atomic representation of the gramicidin backbone but owing to the short simulation times (5 ps), it is possible that their system did not reach equilibrium.

Table 2 illustrates the ion–water separations in different regions of the channel. Na^+ differs distinctly from both Cs^+ and K^+. In the rigid channel, the water's mean distance from the ion is comparable to (and in the case of $\alpha > 0$, somewhat shorter than) that calculated for the gas phase MW_2 complex (2.52 Å). The short Na^+-water separations correlate with the high dipole moments observed for the rigid channel. For Cs^+ and K^+, the separations are much greater than those in the MW_2 complex (3.11 and 2.78 Å respectively); they are closer to values representative of gaseous ion–water tetramer and ion–water hexamer microclusters [54]. The main determinant of the ion–water distance within our channel is naturally the ionic size. There are however, minor differences as we vary the two parameters under study. First of all, as the channel is made increasingly flexible in the absence of polarizability the ion–water distance tends to increase, and more clearly for Na^+ than either of the other two ions. This tendency towards longer ion–water distances is less clearly evident when polarizability is turned on and may even be reversed for Cs^+. Any polarizability dependent differences are only marginally statistically significant when observed from the point of view of regional average values, but there are shifts in the ion–first water distance distributions when seen from the perspective of the entire channel (See Fig. 2). There is a definite polarizability dependent ion–water distance shortening due to switching on polarizability for sodium which is still noted, but less marked, in the case of potassium. For cesium occupancy this effect nearly vanishes; there is really no polarizability dependence on the ion–water distances for the rigid and flexible backbones, but there is a slight shift to shorter distances for the very flexible backbones. Unlike the influence of polarizability, varying channel flexibility leads to only slight shifts in the distribution of ion–water separations, basically only noticeable for sodium.

To summarize, ion–water separations are dominated by the size of the ion. Flexibility tends to expand the average distances somewhat, while dynamical polarizability shortens the distances. The

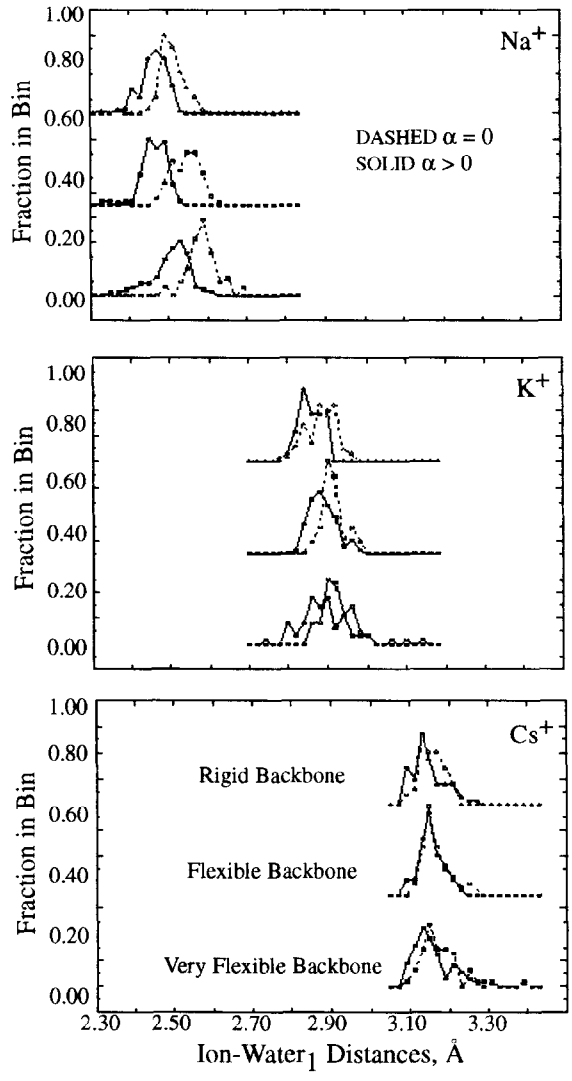

Fig. 2. Comparison of Na^+, K^+, and Cs^+ ion-first water distances. Average ion–water$_1$ distances from each window in all three regions of a given channel type were pooled and binned. The x-axis represents the ion–water distances in Å (left bin edge) and the y-axis indicates the fraction of the total found within that bin (bin size = 0.02 Å). The flexible and rigid channels are offset along the y-axis for easier viewing. Solid lines represent $\alpha > 0$, while the dashed lines depict the $\alpha = 0$ case. It is clear that for sodium switching on polarizability results in shorter ion–water distances for all degrees of backbone flexibility. The effect is still noted, but to a much lesser degree for potassium, and is not exhibited by cesium.

Table 3
Mean water–water separations (in Å) in the vicinity of the ion [a]

	Na^+				K^+				Cs^+			
	$\alpha = 0$		$\alpha > 0$		$\alpha = 0$		$\alpha > 0$		$\alpha = 0$		$\alpha > 0$	
	w_1–w_2	w_2–w_3	w_1–w_2	w_2–w_3	w_1–w_2	w_2–w_3	w_1–w_2	w_2–w_3	w_1–w_2	w_2–w_3	w_1–w_2	w_2–w_3
Rigid	$d_{free}(\alpha = 0) = 3.11 \pm 0.04$							$d_{free}(\alpha > 0) = 3.13 \pm 0.04$				
Junction	3.05 ± 0.04	3.08 ± 0.05	2.97 ± 0.03	3.02 ± 0.04	3.06 ± 0.04	3.11 ± 0.04	3.05 ± 0.04	3.09 ± 0.07	3.07 ± 0.04	3.12 ± 0.02	3.06 ± 0.06	3.08 ± 0.05
Monomer	3.02 ± 0.06	3.07 ± 0.07	2.95 ± 0.05	3.05 ± 0.08	3.03 ± 0.06	3.10 ± 0.05	3.02 ± 0.08	3.08 ± 0.08	3.05 ± 0.06	3.11 ± 0.06	3.03 ± 0.07	3.10 ± 0.08
Exit	3.05 ± 0.04	3.10 ± 0.06	2.93 ± 0.06	3.00 ± 0.06	3.10 ± 0.07	3.18 ± 0.11	3.00 ± 0.07	3.07 ± 0.09	3.06 ± 0.04	3.13 ± 0.08	3.08 ± 0.07	3.13 ± 0.09
Flexible	$d_{free}(\alpha = 0) = 3.13 \pm 0.02$							$d_{free}(\alpha > 0) = 3.15 \pm 0.05$				
Junction	3.08 ± 0.08	3.11 ± 0.06	3.00 ± 0.04	3.04 ± 0.03	3.10 ± 0.05	3.17 ± 0.05	3.10 ± 0.05	3.13 ± 0.03	3.05 ± 0.03	3.14 ± 0.04	3.08 ± 0.05	3.10 ± 0.05
Monomer	3.06 ± 0.06	3.10 ± 0.06	2.99 ± 0.08	3.07 ± 0.07	3.11 ± 0.05	3.17 ± 0.06	3.15 ± 0.09	3.16 ± 0.10	3.07 ± 0.05	3.14 ± 0.04	3.09 ± 0.04	3.12 ± 0.03
Exit	3.08 ± 0.06	3.10 ± 0.05	3.03 ± 0.04	3.07 ± 0.03	3.07 ± 0.06	3.08 ± 0.05	3.12 ± 0.10	3.10 ± 0.08	3.09 ± 0.04	3.14 ± 0.05	3.08 ± 0.06	3.11 ± 0.07
Very flexible	$d_{free}(\alpha = 0) = 3.16 \pm 0.05$							$d_{free}(\alpha > 0) = 3.18 \pm 0.08$				
Junction	3.09 ± 0.08	3.22 ± 0.10	3.04 ± 0.10	3.12 ± 0.12	3.04 ± 0.06	3.15 ± 0.08	2.94 ± 0.05	3.04 ± 0.09	3.07 ± 0.07	3.11 ± 0.06	3.03 ± 0.09	3.11 ± 0.09
Monomer	3.09 ± 0.14	3.17 ± 0.14	3.03 ± 0.12	3.09 ± 0.11	3.09 ± 0.09	3.13 ± 0.07	3.04 ± 0.13	3.13 ± 0.23	3.11 ± 0.06	3.19 ± 0.05	3.12 ± 0.09	3.18 ± 0.09
Exit	3.08 ± 0.06	3.13 ± 0.05	3.01 ± 0.09	3.06 ± 0.11	3.07 ± 0.08	3.07 ± 0.13	3.18 ± 0.13	3.16 ± 0.20	3.09 ± 0.06	3.15 ± 0.09	3.10 ± 0.07	3.13 ± 0.08

[a] Mean water–water distances for first and second water pairs adjacent to Cs^+, K^+, and Na^+ ions in the model channel computed for the three channel regions of interest. In each case the first number is the $water_1$–$water_2$ separation and the second is the $water_2$–$water_3$ distance. Mean water–water distances, d_{free}, in the ion free channel are listed for comparison.

effects are most distinct for sodium, less so for potassium, and virtually absent for cesium.

3.3. Water–water correlations and electrostriction

Several comparisons have been made with respect to inter-water distances among non-exchangeable waters, including full channel and regional comparisons as functions of ion occupancy, flexibility, and polarizability. From Table 3, we first note that in ion-free channels the mean water–water distances depend slightly on polarizability and backbone flexibility, decreasing as the channel becomes more rigid and increasing when polarizability is considered. Fig. 3 presents a general overview of adjacent water–water distances throughout entire ion occupied channels. Mean water–water separations from all windows at the junction, mid-monomer, and exit were pooled and binned for each of the three ions and the distributions normalized and examined. Some overall trends emerge. As the ion gets smaller, the number of very short (< 3.0 Å) water–water separations increases (See Figs. 3 and 4). Making any channel more flexible, not surprisingly, leads to a broadening of the distribution of water–water distances. (See Fig. 4). Shortening of the water–water distances throughout an ion-occupied channel (electrostriction) with respect to water–water distances in an ion free channel is most definitely noted in the case of sodium (See Fig. 3), but only in simulations where $\alpha > 0$. It is weakly observed in the case of potassium. The effect does not occur for cesium under any conditions. Increasing channel flexibility basically tends to negate the ion-induced electrostriction observed when polarizability is switched on. When $\alpha = 0$, the water–water distance distributions for all three ions at each respective flexibility are almost superimposable (See Fig. 4), however the distances are still slightly shorter than those in the corresponding ion free channels, most notably in the rigid and flexible ones. When $\alpha > 0$, however, the Na^+ and K^+ distributions are sharply displaced to shorter water–water distances when the channel is rigid (See Fig. 4). In the flexible model channel, Cs^+ and K^+ water–water distances become approximately the same, with the Na^+ distribution still significantly skewed to shorter separations. With the channels very flexible, all water–water distance distributions are once again nearly

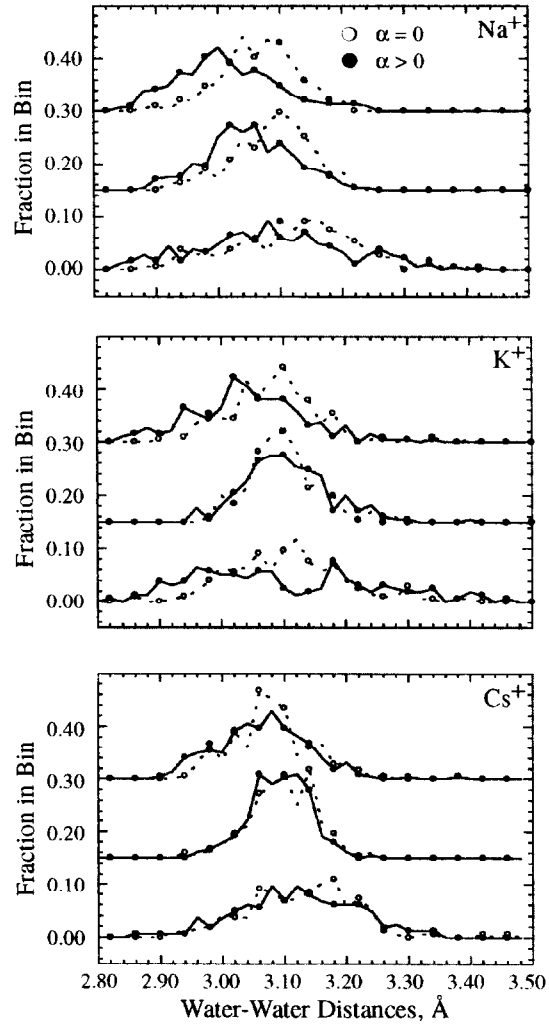

Fig. 3. Comparison of Na^+, K^+, and Cs^+ induced electrostriction. Average water–water distances from each window in all three regions of a given channel type were pooled and binned. The x-axis represents the water–water distances in Å (left bin edge) and the y-axis indicates the fraction of the total found within that bin (bin size = 0.02 Å). The flexible channels are offset along the y-axis by 0.15, and the rigid by 0.30. Solid lines represent $\alpha > 0$, while the dashed lines depict the $\alpha = 0$ case. Electrostriction is very noticeable for rigid and flexible Na^+ channels in the $\alpha > 0$ simulations and absent under identical conditions when Cs^+ occupies the model pore. Some minor electrostriction is evident in the rigid K^+ channel. Not unexpectedly, increasing flexibility broadens the distribution of water–water distances. The dashed lines with open circles refer to $\alpha = 0$ simulations, the solid lines with closed circles, $\alpha > 0$ simulations. Every other bin is marked with a circle.

superposable, as in the $\alpha = 0$ case. In all instances, the water–water distances are distinctly shorter than in the equivalent ion free channel.

The question could be posed as to whether the phenomenon of electrostriction is equally pronounced in each part of the channel, i.e., are the differences in the overall channel pictures comprised of dramatic effects from primarily one channel region with minimal contribution from the others. Fig. 5 addresses this question with a breakdown of results

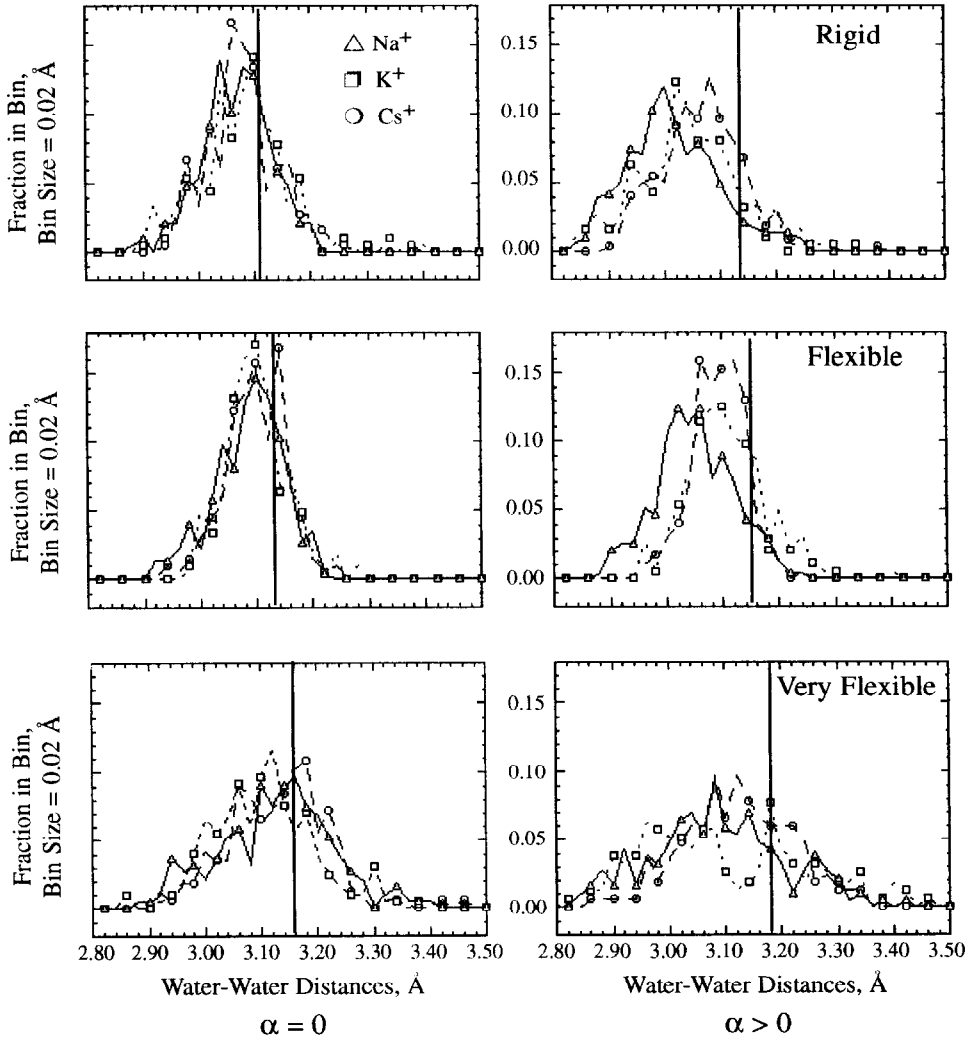

Fig. 4. Effect of backbone flexibility on ion induced electrostriction. The left panels illustrate that in the absence of polarizability, the distributions of the water–water separations for all three ions are virtually indistinguishable; flexibility of the backbone plays no role. When $\alpha > 0$, however, this pattern changes. For the rigid channel, the peak of the sodium distribution is located at 3.00 Å, followed by potassium at 3.02 Å, and cesium at 3.08 Å. All three distributions are broader with respect to $\alpha = 0$. As the channel is made flexible, the K^+ and Cs^+ distributions become superposable, peaking around 3.10 Å, with the sodium channel distribution still skewed to shorter water–water separations. In very flexible channels, all three distributions effectively become superposable again, albeit with some minor skewing of the Na^+ distribution to shorter distances. The vertical line indicates the position of the mean water–water distance in the comparable, ion-free channel. Every other bin is marked with a symbol.

by region for potassium and sodium occupied channels. For both ions, electrostriction is marginally more prominent at the junction and the exit. While it is still noted in the mid-monomer, the distribution is broad and the effect is less clear. Overall it is fair to conclude that no region contributes disproportionately to the shortening of the water–water distances when $\alpha > 0$.

Table 3 focuses more specifically on the $water_1$–$water_2$ and $water_2$–$water_3$ distances of pairs immediately adjacent to the ion. In comparing these numbers to the average water–water distance in the comparable ion free channel, it is clear that the $water_1$–$water_2$ separations are greatly reduced. The effect is strongest for Na^+, more pronounced when $\alpha > 0$ and little dependent on channel flexibility.

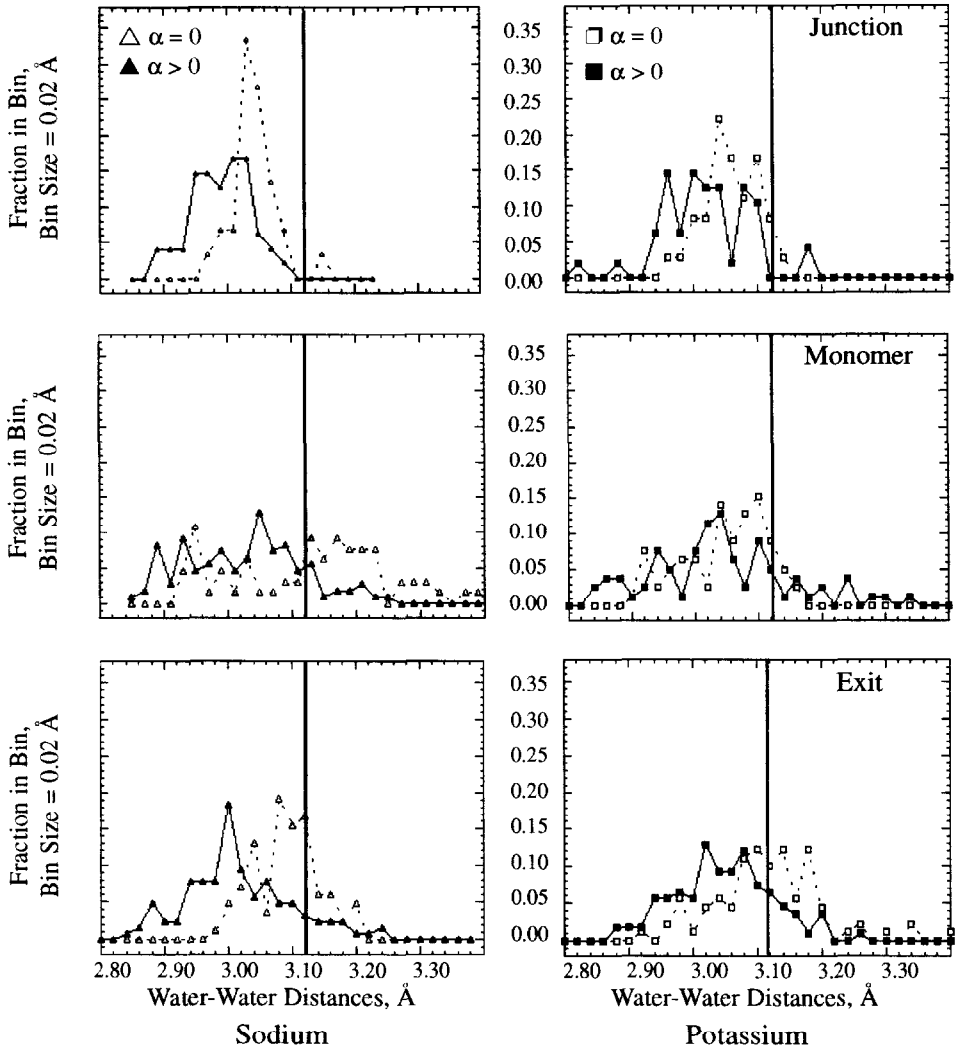

Fig. 5. No channel region contributes disproportionately to the observed electrostriction. A breakdown of water–water distances (in Å) by channel region is presented for Na^+ and K^+ within the rigid channel. Although electrostriction is slightly less pronounced in the mid-monomer and most marked at the junction, it is clearly a phenomenon that occurs throughout the channel and is not restricted to a particular region. Each bin is indicated with a symbol. Vertical line indicates the average water–water distance in rigid, ion-free channels.

When $\alpha \neq 0$, the water$_2$–water$_3$ distances are also noticeably smaller than in the comparable ion-free system. Only when $\alpha = 0$ is there no clear pattern of electrostriction in the water$_2$–water$_3$ separations. Although the statistical variation in channel average values is large, taken together, ion-induced electrostriction is unmistakably apparent when $\alpha > 0$. Considering the mean water$_1$–water$_2$ distances in Na^+ occupied channels, 100% of the values are smaller when polarization is switched on, for K^+ that number falls to two thirds, and for Cs^+, it is just under half. For the water$_2$–water$_3$ distances, all of the values for Na^+ and Cs^+ are smaller when $\alpha > 0$, and for K^+ three-quarters of them are smaller. The rms fluctuations for any particular comparison might make it appear as if there is little difference between $\alpha = 0$ and $\alpha > 0$, especially for the more flexible channels. When viewed as a whole, however, the differences are clearly evident. Binning was performed on the first and second waters only in the same manner as was done for the whole channel and the same overall shifts towards smaller water–water distances were observed as the averages suggest (data not shown).

To summarize, ion induced electrostriction is prominent when the ion is small, polarizability is on, and the channel is rigid. Increasing flexibility attenuates the enhanced electrostriction that is observed when $\alpha > 0$. For K^+ and Na^+, electrostriction occurs both close to and further (3 or more waters away) from the ion. For the largest ion, Cs^+, it is only observed for the first pair of waters adjacent to the ion, not throughout the channel.

3.4. Water–water orientational correlations

Fig. 6 illustrates other significant effects that cation variation has on the properties of water in various channel regions. In fact, orientational correlation is conceivably a significant means by which occupancy information is communicated across the channel. For these panels the x-axis refers to the position of the water with respect to the ion in the single file along the channel axis. Zero indicates the location of the ion, with the positive values being the water neighbors ahead of the ion, and the negative numbers, those waters trailing the ion. One is the nearest neighbor, two the next nearest, etc. The y-axis represents the angle of the μ vector with the channel axis. A 0° orientation indicates perfect alignment, while 90° indicates complete loss of orientational correlation. Uncertainties are in the range of 5–10°, with the lower value referring to those waters closest to the ion. Uncertainties increase as distance from the ion increases.

The first panel of each column shows orientations when the ion is located near the junction. Correlation is lost most readily in the very flexible case. The loss occurs slightly more slowly when $\alpha = 0$ in the cases of Cs^+ and K^+, but this effect is not an important factor for Na^+. Overall, for the Na^+ occupied channel the water remains most aligned, both close to and far from the ion, at all flexibilities and with polarizability on or off. Water's behavior in the K^+ and Cs^+ occupied channel is very similar in terms of loss of correlation and is distinct from that in the Na^+ occupied channel. With an ion at mid-monomer, depicted in the center panels, the same basic pattern is seen as at the junction, with only minor differences. Here, again, long range correlation is more persistent when $\alpha = 0$. The effect is more notable for the Cs^+ and K^+ occupied channels than for those occupied by Na^+; with Na^+ present water again remains more correlated than when the larger ions are the permeating species. At the exit, illustrated in the bottom panels, the same pattern is noted. As expected, correlation is minimal four waters removed from the ion (a cut-off of 9.5 Å was used). Channels occupied by Cs^+ and K^+ show greater loss of correlation than with Na^+ present in a rigid channel. Effectively, this means that an ion about to enter a channel at the left mouth would see a water environment more similar to an empty channel with a Cs^+ or K^+ ion in the right hand mouth than it would with Na^+ in that same position.

To summarize, increasing channel flexibility correlates negatively with the propagation of dipolar correlations as measured by water dipole orientations. The effect is noted for all three alkali cations. The water chain is most highly correlated for any degree of flexibility with Na^+ as permeant and the least highly correlated with Cs^+ present; K^+ is roughly intermediate. Setting $\alpha = 0$ weakly promotes retention of long range orientational correlation, especially for the larger ions.

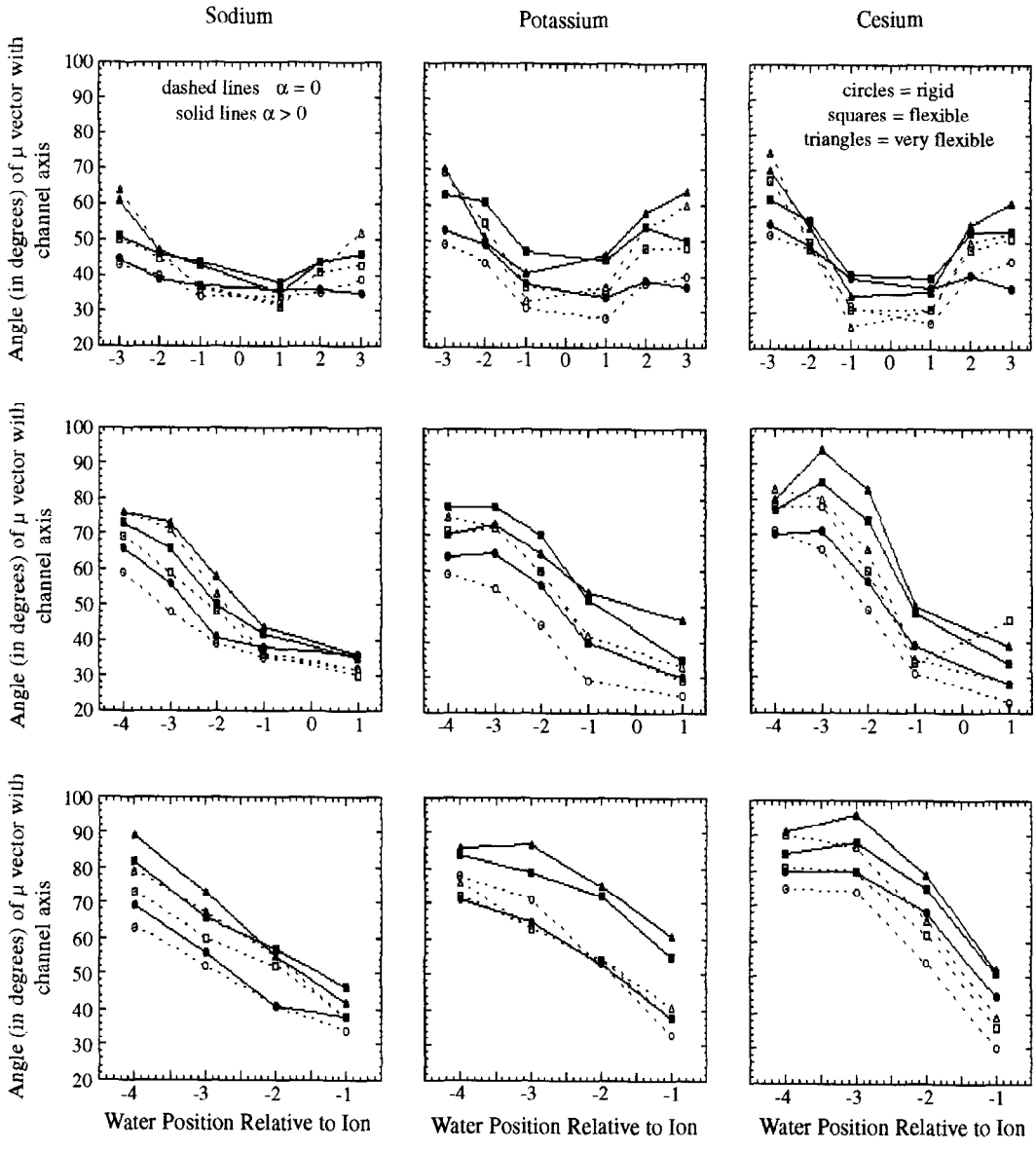

Fig. 6. Long-range orientational correlation persists for Na^+ and is rapidly lost for Cs^+, with K^+ being intermediate to them. The x-axis designates the position of water molecules with respect to the ion. The zero position indicates the location of the ion, with negative values representing consecutive waters to the left of the ion within one gramicidin monomer, and positive values, consecutive waters to the right of the ion in the channel. The y-axis is the angle (θ in degrees) that the z component of the water dipole moment makes with the channel axis. Each point represents the channel average of all $\cos\theta$ for the particular location relative to the ion; for waters to the right of the ion, $\theta = \cos^{-1}\{|\Sigma\cos\theta_i|/n\}$ in order to keep the scale the same for both sides of the ion. A 0° orientation indicates perfect alignment; 90° denotes complete loss of correlation. For all three ions rigidity of the backbone favors retention of long range correlation. Not allowing the dipole moments to fluctuate about their mean values slightly enhances retention of long range correlation, especially for the larger ions. The top panels refer to an ion at the junction; middle, mid-monomer; and bottom, exit.

4. Discussion

Conventional biomolecular force fields assign channel and bulk water the same mean monomer behavior, despite vastly different surroundings. Water within the channel is strongly polarized by the field of an ion, yet the requirement of single filing imposed by gramicidin's small diameter greatly alters its orientational response to the field of an ion [65]. Likewise polar channel groups are influenced by the ionic field, albeit less strongly. We have pursued an approach incorporating non-additivity so that mean monomer properties of water can differ depending on environment. We consider the consequences of instantaneously polarizable groups on the pore waters' electrical properties, water–water, and ion–water correlations with special emphasis on long range correlations capable of propagating occupancy information.

The specific question we examined was whether allowing instantaneous readjustment of the magnitude of the waters' and the channel groups' dipole moment vectors would substantially alter the channel waters' behavior relative to the scenario where these quantities were fixed at average values. Some early simulations of MacKay et al. [12], Skerra and Brickman [3], and Chiu et al. [15] which focussed particularly on the nature of the water structure within the channel employed potential functions where channel water possessed 'average' properties. In such simulations, water tends to maintain rather long range correlations, despite the possibility of occasional gaps which transiently emerge in the chain. In such channels a clear means exists for the transmission of information, namely the orientation of the water molecules' dipoles. Our results show that this mechanism generally does not exist unless the backbone remains extremely rigid.

We demonstrate three features resulting from the incorporation of polarizability into the potential function that have significant implications for intra-channel information transfer: (1) ion–water distances tend to shorten, especially for smaller ions and in a region-specific manner; (2) electrostriction (shorter water–water distances) is observed, notably for the smaller ions; and (3) loss of orientational correlation occurs more rapidly when $\alpha > 0$, for all three ions, but most notably for cesium. This last result is especially important as part of a potential mechanism for cation-specific induced changes in water structure. A scrambling of water–dipole correlations is much more pronounced for the cesium ion than for the sodium ion. Roux et al. [28] using a full atomic representation of gramicidin incorporating polarizable peptide groups and TIP3P waters in a molecular dynamics simulation have studied the basis for double vs. single occupancy of the gramicidin channel. Although their system did not include fully polarizable water, they find that loss of favorable water–ion interactions within the channel is responsible for the greater tendency of the larger ions to doubly occupy gramicidin. This observation is certainly consistent with our result concerning ion–induced water ordering. Sodium polarizes its nearest neighbor water molecules more strongly than do the other ions and this effect propagates throughout the entire length of the channel. Water molecules are better oriented both close to and far from the sodium than with either of the two larger cognates. The net result is that a water molecule in the left hand mouth of the channel is much more sensitive to the presence of a sodium ion on the other side of the channel than it is to the presence of either cesium or potassium, especially if the channel is rigid. With sodium anywhere in the channel, the water molecules are well aligned and it must be harder to effect the water reorientation needed to bind a second sodium (or any other cation).

It is well established experimentally that altering membrane fluidity has a dramatic effect on many single channel properties, among them conductances and open channel lifetimes [66,56]. By modulation of the degree of backbone flexibility, we are attempting to mimic the range of lipid environments that the gramicidin dimer experiences. Backbone motions have implications for cross channel information transfer as well. It has been shown experimentally that there is a time scale coincidence between ionic transport and gramicidin backbone motions [32]. Certainly factors that would contribute to the destabilization of the β-helices would disrupt ionic translocation. On the other hand, locking the backbone into an absolutely rigid state would tend to underestimate the protein–water interactions that contribute significantly to the transport process.

As the absolute degree of motion the entire channel enjoys when embedded in a lipid matrix is

unknown, we have taken the approach of examining the backbone with three degrees of motional restraint, viz. rigid, flexible, and very flexible. Both native and modified gramicidin has been embedded in a variety of membrane environments of variable fluidity. Gramicidin groups must have some flexibility in order to facilitate transport, yet enough structural stability to present an open permeation pathway to diffusing species. The experimental record suggests that gramicidin may fall somewhere between the rigid and flexible scenarios we present [56].

There are several features we note as the channel is made more flexible: (1) water–dipole moments tend to drop in an ion-specific way; (2) the number of non-exchangeable waters in the single file regime drops, as exchange with the bulk becomes rapid; (3) ion–water distances expand slightly; (4) water–water distance distributions tend to broaden and shift towards larger separations, again in an ion specific way; and (5) long range orientational correlation is rapidly lost. The effects of flexibility are most pronounced on cesium and least so on sodium, with potassium representing an intermediate case.

Our work differs from a number of previous studies with respect to the manner in which membrane fluidity is approximated. In the present model all groups are tethered to the 0 K positions, but none is fixed. By reducing the value of the tethering force constant we obtain a range of backbone flexibilities, while many early simulations simply localized the C_αs to their 0 K positions. This particular feature alone was probably sufficient to suggest much longer orientational correlations that we have found in our present study. Chiu et al. [25] have examined the effects of backbone flexibility in molecular dynamics simulations where the helical form was maintained by artificial restraints on the peptide's helical form. By varying the characteristic time constant of the restraints they were able to mimic a wide range of backbone flexibilities. However, they were using a standard biomolecular force field for their calculations (GROMOS) and an ion-free channel. They found that even in flexible channels a fairly long range water correlation could be observed, although transient breaks in the single file chain emerged. Their rigid channels, however, seemed to 'trap' water and freeze further motion.

The effects of increasing flexibility are quite as would be expected and monotonic in the tendency toward loss of long range correlation, from the point of view of both increased ion–water and water–water distances and of loss of ordering of water dipole moment vectors. The effects that incorporating polarizability in the potential function have on long range correlation are more complex. Viewed from the perspective of shortened ion–water and water–water distances, $\alpha \neq 0$ indeed tends to foster longer ranged correlations within channels. On the other hand, presumably due to enhanced ion–water–peptide group interactions, the orientation of the water dipole moments becomes more random thereby reducing long range correlation. These two effects appear contradictory, but in fact are really not when one considers the degree to which each occurs and in which channels. The loss of orientation of the water dipole moments is most pronounced when the ionic radius is large and, in these cases, the ion–water and water–water distances are larger at the outset. Given that the larger ions are less able to polarize water, especially when relatively more highly co-ordinated with channel carbonyls, H_2O molecules are more available for interaction with the backbone groups. In each case, the effect is more dramatic as the distance from the ion increases; once again, as ionic ability to polarize water wanes, opportunities for interaction with the gramicidin channel increases. Finally, loss of orientation is relatively greater at the exit than in either of the other two regions. Greater ionic coordination to available carbonyls reduces the ion's ability to orient the distant water molecules. The conclusion to be drawn from these results is simply that the incorporation of polarizability has dramatic effects on the electrical properties of water, the relative degree of water–ion vs. water–peptide interaction, and the capacity of the water chain to serve as an information conduit. The implications of channel flexibility are much more straightforward and predictable; the challenge is in identifying the appropriate degree of flexibility corresponding to any given membrane environment.

5. Summary

Some clear patterns emerge from the results just presented. Smaller ions, rigid channel backbones,

and polarizability generally contribute to stronger ion–water and water–water interactions in our model system. Specifically, as the channel becomes more rigid both ion–water and water–water correlations are affected: in the $\alpha > 0$ simulations water dipole moments are larger and ion–water distances decrease; there is electrostriction (water–water distances decrease); long range orientational correlation of the water molecules is more persistent. Incorporating polarizability affects ion–water and water–water correlations differently: ion–water distances shorten and electrostriction is observed; long range orientational correlation of the waters is, however, weakened. As the ionic radius decreases, there is greater electrostriction and more persistent water–water orientational correlation. Both group polarizability and backbone flexibility have an effect on channel water properties. The effect of flexibility is global, monotonic in nature, and independent of ionic identity, whereas that of polarizability is more complex and a function of several variables, i.e., ionic identity, location of ion in the channel, and location of the water with respect to the ion.

Acknowledgements

This work has been supported by a grant from the National Institutes of Health (GM-28643) and by grants of computer time from the Pittsburgh Supercomputer Center.

References

[1] B. Hille, Ionic Channels of Excitable Membranes, 2nd Edn. (Sinauer Associates, Sunderland, MA, 1992).
[2] A. Finkelstein and O.S. Andersen, J. Membr. Biol. 59 (1981) 155.
[3] A. Skerra and J. Brickmann, Biophys. J. 51 (1987) 969.
[4] B. Roux and M. Karplus, Biophys. J. 59 (1991) 961.
[5] S. Bogusz and D. Busath, Biophys. J. 62 (1992) 19.
[6] V. Dorman, M.B. Partenskii and P.C. Jordan, Biophys. J. 70 (1996) 121.
[7] D. Urry, Int. Rev. Neurobio. 21 (1979) 311.
[8] N. Unwin, J. Mol. Biol. 229 (1993) 1101.
[9] O.S. Andersen, Ann. Rev. Physiol. 46 (1984) 531.
[10] D.D. Busath, Ann. Rev. Physiol. 55 (1993) 473.
[11] O.S. Andersen and R.E. Koeppe II, Physiol. Rev. 72 (4) (1992) S89.
[12] D.H.J. Mackay, P.H. Berens, K.R. Wilson and A.T. Hagler, Biophys. J. 46 (1984) 229.
[13] K.S. Kim and E. Clementi, J. Am. Chem. Soc. 107 (1985) 5504.
[14] J. Åqvist and A. Warshel, Biophys J. 56 (1989) 171.
[15] S.W. Chiu, S. Subramanian, E. Jakobsson and J.A. McCammon, Biophys. J. 56 (1989) 253.
[16] B. Roux and M. Karplus, J. Phys. Chem. 95 (1991) 4856.
[17] B. Roux and M. Karplus, J. Am. Chem. Soc. 115 (1993) 3250.
[18] B.W. Urban, S.B. Hladky and D.A. Haydon, Federation Proc. 27 (12) (1978) 2628.
[19] B.W. Urban, S.B. Hladky and D.A. Haydon, Biophys. Biochim. Acta 602 (1980) 331.
[20] G.A. Olah, H.W. Huang and W. Liu, J. Mol. Biol. 218 (4) (1991) 847.
[21] K.W. Wang, S. Tripathi and S.B. Hladky, J. Membr. Biol. 143 (3) (1995) 247.
[22] M. Sancho, M.B. Partenskii, V. Dorman and P.C. Jordan, Biophys. J. 68 (1995) 427.
[23] D.P. Chen and R.S. Eisenberg, Biophys. J. 64 (1993) 1405.
[24] D.P. Chen and R.S. Eisenberg, Biophys. J. 65 (1993) 727.
[25] S.W. Chiu, E. Jakobsson, S. Subramaniarn and J.A. McCammon, Biophys. J. 60 (1991) 273.
[26] S.W. Chiu, J.A. Novotny and E. Jakobsson, Biophys. J. 64 (1993) 98.
[27] M. Poxleitner, J. Seitz-Beywl and K. Heinzinger, Z. Naturforsch. 48 C (1993) 654.
[28] B. Roux, B. Prud'hom and M. Karplus, Biophys. J. 68 (1995) 876.
[29] B. Roux, Chem. Phys. Lett. 212 (1993) 231.
[30] R. Elber, D.P. Chen, D. Rojewska and R. Eisenberg, Biophys. J. 68 (1995) 906.
[31] M.D. Becker, R.E. Koeppe II and O.S. Andersen, Biophys. J. 62 (1991) 25.
[32] C.L. North and T.A. Cross, Biochem. 34 (1995) 5883.
[33] A.S. Arseniev, V.E Bystrov, T.V. Ivanov and Y.A. Ovchinnikov, FEBS Lett. 186 (1985) 168.
[34] A.S. Arseniev, I.L. Barsukov, and V.E Bystrov, in Y.A. Ovchinnikov, W. Voelter, E. Bayer and T.V. Iranov (Editors), Chemistry of Peptides and Proteins, Vol. 3 (Voelter, Berlin, 1986) p. 127.
[35] B.S. Cornell, E Separovic, A.J. Baldassi and R. Smith, Biophys. J. 53 (1988) 67.
[36] L.K. Nicholson and T.A. Cross, Biochem. 28 (1989) 9379.
[37] R.R. Ketchem, W. Hu and T.A. Cross, Science 261 (1993) 1457.
[38] W.K. Lee and P.C. Jordan, Biophys. J. 46 (1984) 805.
[39] P.C. Jordan, J. Phys. Chem. 91 (1987) 6582.
[40] P.C. Jordan, Biophys. J. 58 (1990) 1133.
[41] S.S. Sung and P.C. Jordan, Biophys. J. 51 (1987) 661.
[42] W. Hu, K.C. Lee and T.A. Cross, Biochemistry 32 (1993) 7035.
[43] D.B. Sawyer, R.E. Koeppe II and O.S. Andersen, Biochem. 28 (1989) 6571.
[44] R.E. Koeppe II and M. Kimura, Biopolymers 23 (1984) 23.
[45] P.C. Jordan, in A. Pullman, J. Jortner and B. Pullman

(Editors), Transport through Membranes: Carriers, Channels and Pumps (Kluwer, Dordrecht, 1988) p. 237.
[46] C.Y. Lee, A. McCammon and P.J. Rossky, J. Chem. Phys. 80 (1984) 4448.
[47] B.R. Brooks, R.E. Bruccoleri, B.D. Olafson, D.J. States, S. Swaminathan and M. Karplus, J. Comp. Chem. 4 (1983) 187.
[48] S.J. Weiner, P.A. Kollman, D.A. Case, U.C. Singh, C. Ghio, G. Alagone, S. Profeta and P. Weiner, J. Am. Chem. Soc. 106 (1984) 756.
[49] J. Hermans, H.J.C. Berendsen, W.F. van Gunsteren and J.P.M. Postma, J. Comp. Chem. 23 (1984) 1513.
[50] K.A. Duca and P.C. Jordan, Biophys. J. 64 (1993) 301a.
[51] P. Barnes, J.L. Finney, J.D. Nicholas and J.E. Quinn, Nature 282 (1979) 459.
[52] B.J. Gellatly, J.E. Quinn, P. Barnes and J.L. Finney, Mol. Phys. 50 (1983) 949.
[53] S.S. Sung and P.C. Jordan, J. Chem. Phys. 85 (1987) 4045.
[54] S. Lin and P.C. Jordan, J. Chem. Phys. 89 (1988) 7492.
[55] S.H. Heinemann and F. Sigworth, Biophys. J. 57 (1990) 499.
[56] J.A. Killian, Biochim. Biophys. Acta 1113 (1992) 391.
[57] K. He, S.J. Ludtke, Y. Wu, H.W. Huang, O.S. Andersen, D. Greathouse and R.E. Koeppe II, Biophys. J. 49 (1994) 83.
[58] H.J.C. Berendsen, J.P.M. Postma, W.F. van Gunsteren, A. DiNola and J.R. Haak, J. Chem. Phys. 81 (1985) 3684.
[59] C.W. Gear, Numerical Initial Value Problems in Ordinary Differential Equations (Prentice-Hall, Englewood Cliffs, NJ 1971).
[60] D.J. Evans and S. Murad, Mol. Phys. 34 (1977) 327.
[61] P.A. Rosenberg and A. Finkelstein, J. Gen. Physiol. 72 (1978) 327.
[62] D.G. Levitt, S.R. Elias and J.M. Hautman, Biochim. Biophys. Acta 512 (1978) 436.
[63] D.G. Levitt, in W.D. Stein (Editor), Ion Channels: Molecular and Physiological Aspects (Academic Press, New York, 1983).
[64] K.S. Kim, D.P. Vercauteren, M. Welti, S. Chin and E. Clementi, Biophys. J. 47 (1985) 327.
[65] M.B. Partenskii and P.C. Jordan, J. Phys. Chem. 96 (1992) 3906.
[66] K.J. Cox, C. Ho, J.V. Lombardi and C.D. Stubb, Biochem. 31 (1992) 1112.